

## The Effect of Annealing to the Hardness of High $Y_2O_3$ -Oxide Dispersion Strengthened (ODS) Ferritic Steels

(Kesan Sepuh Lindap terhadap Kekerasan Keluli Ferit ODS- $Y_2O_3$  Tinggi)

FARHA MIZANA SHAMSUDIN\*, SHAHIDAN RADIMAN, YUSOF ABDULLAH & NASRI A. HAMID

### ABSTRACT

*The purpose of this study was to investigate the effect of annealing to the hardness of high  $Y_2O_3$ -oxide dispersion strengthened (ODS) ferritic steels. The samples were prepared by mechanical alloying method followed by Cold Isostatic Pressing (CIP). After compaction process, the samples were sintered at 1100°C for 1 h in a tube furnace. The crystal structure and morphology of samples were analyzed by X-ray Diffraction (XRD) measurement and characterized by using field emission scanning electron microscope (FESEM), respectively. The hardness of samples was measured by using a micro-Vickers hardness tester with a load of 200 gf at annealing temperature of 600°C, 800°C and 1000°C, respectively. The Vickers hardness value (HV0,2) versus annealing temperature graph showed that the hardness of all samples started to decrease at temperature of 600°C due to grain growth. The hardness value of all samples (1Y and 5Y) identified at this annealing temperature is 855 HV0,2 and 808 HV0, 2, respectively.*

*Keywords: Electron microscopy; hardness measurement; mechanical alloying; ODS ferritic steel; XRD measurement*

### ABSTRAK

*Tujuan kajian ini dijalankan adalah untuk mengkaji kesan sepuh lindap terhadap kekerasan keluli ferit ODS- $Y_2O_3$  tinggi. Sampel bagi kajian ini telah dibangunkan dengan menggunakan kaedah pengalioian mekanik dan diikuti dengan kaedah Tekan Isostasi Sejuk (CIP). Selepas proses pemampatan, sampel didedahkan dengan rawatan haba pada suhu 1100°C selama 1 jam di dalam relau pembakaran. Struktur kristal dan morfologi sampel masing-masing telah dianalisis dengan menggunakan Meter Belauan Sinar-X (XRD) dan dicirikan dengan menggunakan mikroskop elektron pengimbas pancaran medan (FESEM). Kekerasan sampel pula telah diukur dengan menggunakan alat pengukur mikro-Vickers dengan beban sebanyak 200 gf masing-masing untuk suhu sepuh lindap pada 600°C, 800°C dan 1000°C. Graf nilai kekerasan Vickers (HV0,2) melawan suhu sepuh lindap bagi semua sampel telah mendedahkan bahawa kekerasan bagi semua sampel mula menurun pada suhu 600°C disebabkan oleh fenomena pembesaran zarah. Nilai kekerasan untuk semua sampel (1Y dan 5Y) yang telah dikenal pasti pada suhu sepuhlindap ini (600°C) adalah masing-masing sebanyak 855 HV0,2 dan 808 HV0,2.*

*Kata kunci: Keluli ferit ODS; mikroskop elektron; pencirian XRD; pengalioian mekanikal; pengukuran kekerasan*

### INTRODUCTION

Oxide dispersion strengthened (ODS) ferritic steel has been selected as a candidate material for long-life cladding tubes and core structures for future fission nuclear reactor (Gen IV) especially for supercritical-water-cooled reactor (SCWR) and sodium-cooled fast reactor (SFR) (Gelles 1996; Kim et al. 2016; NEA 2014). This iron-based ODS steel containing nano-scale oxide particles usually  $Y_2O_3$  were first introduced and prepared by using mechanical alloying methods (Fischer 1978). This kind of material shows remarkable tensile and creep properties (Alinger et al. 2002; Hayashi et al. 2008; Klueh et al. 2002; Ukai et al. 2002, 1993), possess higher radiation-induced swelling resistant (Li et al. 2014; McClintock et al. 2009; Miller & Zhang 2011) and high thermal stability (Boulnat et al. 2013; Ukai et al. 2002) due to the presence of nano-scale oxide particles within the steel matrix (Hoeltzer et al. 2007; Miao et al. 2008; Susila et al. 2011).

These  $Y_2O_3$  nanoparticles are highly stable at processing and operating temperature due to the negative heat of formation as well as high melting point which is 2425°C (Zakine et al. 1996). In addition, the nano-size  $Y_2O_3$  particles could act as 'filters' to trap helium atoms and its point defects, thus retarding the radiation-induced materials degradation and radiation swelling (Li et al. 2014; McClintock et al. 2009; Miller & Zhang 2011). As this material contains nano-scale oxide strengthening particles or dispersoids which is  $Y_2O_3$ , the thermal stability as well as the operating temperature in future fission nuclear reactor could be increases up to 700°C (NEA 2014). Nano-scale  $Y_2O_3$  particles with size between 10-20 nm and volume fraction of 0.2-0.5 wt. % were usually added according to the published literatures on ODS ferritic steels.

The use of micron-size and nano-size of  $Y_2O_3$  particles with volume fraction between 0.2-0.5 wt. % has been already studied for ODS ferritic steel regarding

their microstructural characteristics and changes, creep behavior, tensile strength and resistant to radiation-induced swelling. However, the hardness behavior of high  $Y_2O_3$ -ODS ferritic steels at various elevated temperature are never been reported. It is worth to understand the hardness behavior of this material at high temperature as it presents the mechanical properties and it will surely affected following the operating temperature. One way to understand the mechanism of thermal stability and hardness of this kind of material is by thermal exposure treatment which is annealing at various high temperatures. The use of high  $Y_2O_3$  content which is more than usual for the sample in this present study was to examine the formation of dispersoids as well as to identify the hardness at high temperature. Thus, the purpose of this present study was to investigate the effect of annealing at various elevated temperatures to the hardness of high  $Y_2O_3$ -ODS ferritic steel.

#### MATERIALS AND METHODS

High purity elemental powders of iron (Fe), chromium (Cr) and yttria ( $Y_2O_3$ ) were weighed separately in a glove box filled with pure argon atmosphere and mixed according to the compositions as in Table 1. The mixed powder was then sealed in a planetary ball mill Pulverisette 7 milling jar and the mechanical milling process was carried out at 350 rpm for 15 h. The ball-to-powder weight ratio (BPR) is 5:1. After mechanical milling process, the milled steel powder were compacted into green body (bulk shape) via die compaction method with 250 MPa pressure and then followed by Cold Isostatic Pressing (CIP) method

with 300 MPa pressure as a secondary operation. Further process was sintering the ODS ferritic steel green bodies at temperature of 1100°C for 1 h in a tube furnace filled with argon gas and the samples were allowed to cool inside.

The crystal structure and morphology of ODS ferritic steel samples were analyzed by using X-ray Diffraction (XRD) (Bruker D8 Advance) and characterized by field emission scanning electron microscope (FESEM) (Carl Zeiss Merlin), respectively. The samples were then annealed at temperature of 600°C, 800°C and 1000°C for 5 h in a tube furnace filled with argon gas prior to the hardness test. The annealed samples were then polished by using 180 grit SiC abrasive papers to remove the external parts until the desired shining surface. The hardness measurement of polished samples was carried out by using a micro-Vickers hardness tester EW422-DAT testing system with a load of 200 gf.

#### RESULTS AND DISCUSSION

The crystal structure of 1Y and 5Y ODS ferritic steel samples obtained from XRD measurement is illustrated in Figure 1. The morphology of 1Y and 5Y ODS ferritic steel samples characterized by FESEM is illustrated in Figure 2(a) and 2(b), respectively. FESEM characterization was utilized to examine the morphology as well as the dispersion and incorporation state of dispersoids within both samples matrix. The precipitates size of dispersoids within both samples matrix measured from SmartTiff software of FESEM is illustrated in Figure 3(a) and 3(b), respectively.

Vickers hardness value ( $HV_{0.2}$ ) versus annealing temperature at 600°C, 800°C and 1000°C, respectively,

TABLE 1. Compositions of ODS ferritic steel samples (wt. %)

Sample	Designation	Fe	Cr	Y2O3
Fe-12Cr-1Y2O3	1Y	Balance	12	1
Fe-12Cr-5Y2O3	5Y	Balance	12	5

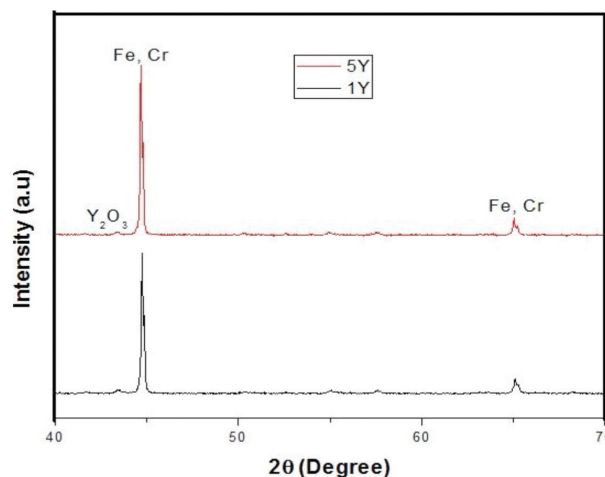


FIGURE 1. Crystal structure of 1Y and 5Y ODS ferritic steel samples

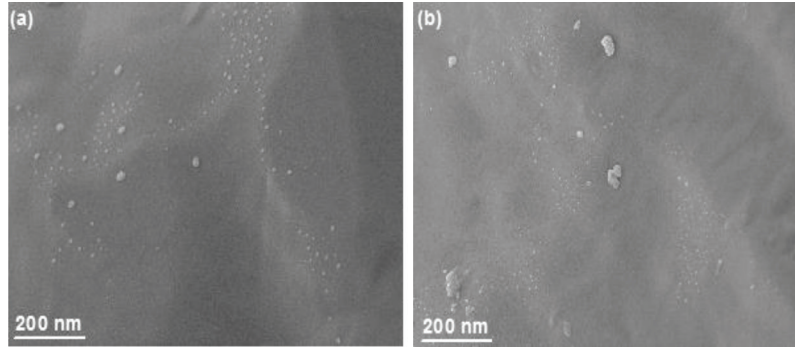


FIGURE 2. Morphology of ODS ferritic steel samples after CIP and sintering (a) 1Y and (b) 5Y

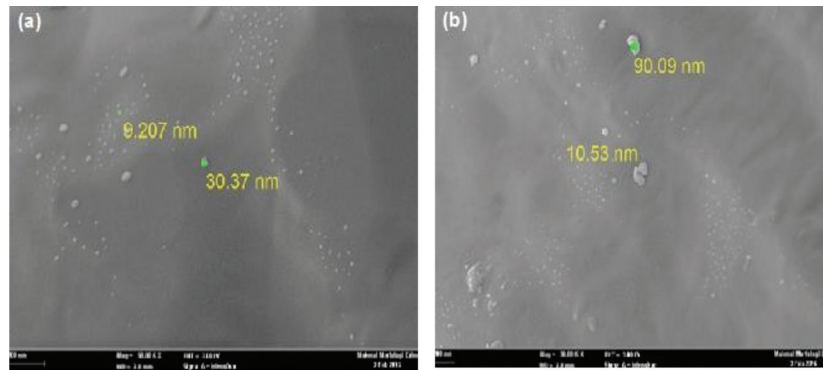


FIGURE 3. Precipitates size of  $Y_2O_3$  nanoparticles dispersion (a) 1Y (b) 5Y

for both samples (1Y and 5Y) is presented in a graph as shown in Figure 4. The hardness of samples reported in this present study demonstrates the behavior and ability of this kind of material to resist plastic deformation at various high temperatures. As the ODS ferritic steels possess remarkable mechanical properties such as high tensile and creep strength as reported in the published literatures, this material surely possess extremely hard surface and strength. Thus, micro-Vickers hardness test is the standard method to measure the hardness of this material compared to other hardness measurement method such as Rockwell and Brinell.

#### CRYSTAL STRUCTURE AND MORPHOLOGY OF SAMPLES

The crystal structure or XRD patterns of 1Y and 5Y ODS ferritic steel samples obtained in this present study are similar to each other and consist of sharp peaks which is consistent with their finishing processing condition after consolidation (compaction and sintering). In comparison with JCPDS data card (PDF 01-081-9987), the main diffraction peaks of both samples can be well indexed to iron (Fe) and chromium (Cr) which confirmed the complete solution of Cr into Fe lattice after 15 h milling time. Also, there is a peak of  $Y_2O_3$  which is the result of their dispersion and incorporation within the sample matrix as

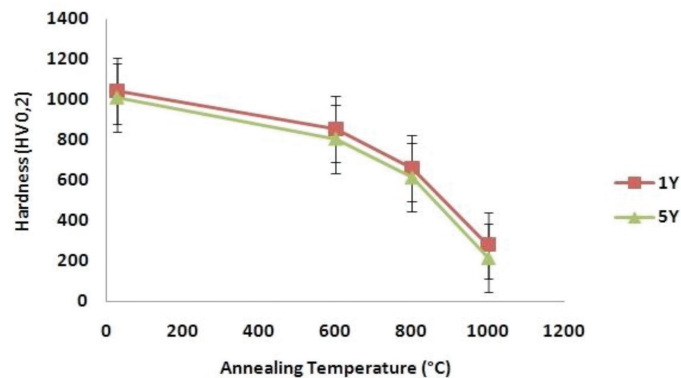


FIGURE 4. Graph of Vickers hardness value (HV0,2) versus annealing temperature of ODS ferritic steel samples (1Y and 5Y)

demonstrated in Figure 1. The crystallite size and density of Fe-12Cr-1Y<sub>2</sub>O<sub>3</sub> ODS ferritic steel (1Y) sample measured from XRD patterns were found to be ~58.17 nm and 7.767 g/cm<sup>3</sup>, respectively. For Fe-12Cr-5Y<sub>2</sub>O<sub>3</sub> (5Y) sample, the crystallite size and density measured from XRD patterns are ~93.21 nm and 7.767 g/cm<sup>3</sup>, respectively.

The FESEM image of both ODS ferritic steel samples are consist of dispersoids formations as illustrated in Figure 2(a) and 2(b), respectively. These formations indicate the dispersion and incorporation state of oxide (nano scale Y<sub>2</sub>O<sub>3</sub> particles) within the samples BCC matrix. Basically, the formation of these dispersoids within the sample matrix is influenced by the solubility equilibrium of O element in the matrix. In other words, the formation of dispersoids in ODS ferritic steel matrix is triggered by the oxidation reaction resulted from the energy change as reported by Williams et al. (2013). FESEM image of 1Y (Fe-12Cr-1Y<sub>2</sub>O<sub>3</sub>) shows the formations of dispersoids within the sample matrix with the precipitates size between 9 and 30 nm as illustrated in Figure 3(a). Whereas 5Y (Fe-12Cr-5Y<sub>2</sub>O<sub>3</sub>) sample exhibit larger precipitates size of dispersoids which is between 10 and 90 nm compared to 1Y sample. Non-uniform precipitates size exhibited by both samples is due to the formation of dispersoids nanoclusters with the size larger than 30 nm within their matrix.

#### HARDNESS (HV0,2) OF ODS FERRITIC STEEL SAMPLES

The plot clearly shows that Vickers hardness value (HV0,2) of two ODS ferritic steel samples (1Y and 5Y) decrease as the annealing temperature increase. 1Y (Fe-12Cr-1Y<sub>2</sub>O<sub>3</sub>) sample possess highest hardness value at all annealing temperature followed by 5Y (Fe-12Cr-5Y<sub>2</sub>O<sub>3</sub>) which is consistent with their morphologies differences. The hardness value of both samples is very high at room temperature (before annealing) which is 1045 HV0,2 for 1Y sample and 1012 HV0,2 for 5Y sample respectively. As the annealing temperature increase up to 600°C, the hardness of both samples started to decrease slightly which is near the limit for this kind of material due to grain growth. At temperature of 600°C, the hardness of 1Y and 5Y identified is about 855 HV0,2 and 808 HV0,2, respectively. Once dispersed within samples matrix, the strengthening dispersoids will exert the pinning pressure known as Zener pinning to prevent grain growth at very high temperature. When the samples is annealed or exposed to high temperature, the energy in their lattice structure increases and forces the grain to growth and enlarges as reported by Pei 2013. When the annealing temperature increases up to 800°C and 1000°C, the hardness of both samples decreases rapidly down in the range of 700 HV0,2 to 200 HV0,2. The hardness of 1Y and 5Y samples identified at 1000°C is 280 HV0,2 and 217 HV0,2, respectively. At this annealing temperature, the strengthening dispersoids within both samples matrix exhibit coarsening as it exposed to very high temperature. This phenomenon known as Ostwald-ripening which has been triggered by the chemical potential differences

related to the energy in lattice structure that will increase once it exposed to very high temperature (Williams et al. 2013).

Direct comparison with the hardness behavior of other ODS ferritic steel samples is not possible since the same amount of Y<sub>2</sub>O<sub>3</sub> nanoparticles dispersed and indenter load were not available in the published literatures. Nevertheless, it is worth to remark that the hardness behavior of ODS ferritic steel is influenced by the annealing temperature as reported by Saber et al. (2014). The hardness behavior of ODS ferritic steel samples (1Y and 5Y) identified in this present study is consistent with the one reported by Saber et al. (2014), which stated that the hardness of this kind of material decreased as the annealing temperature increase due to grain growth and coarsening of dispersoids. In this present study, it is also worth to remark that the hardness of ODS ferritic steel does not influenced by the amount of Y<sub>2</sub>O<sub>3</sub> nanoparticles added and dispersed within its matrix. 1Y sample which contain 1 wt. % of Y<sub>2</sub>O<sub>3</sub> nanoparticles possess high hardness compared to 5Y sample which contain 5 wt. % of Y<sub>2</sub>O<sub>3</sub> nanoparticles as shown in this study. Lower amount of Y<sub>2</sub>O<sub>3</sub> nanoparticles is recognized to generate more fine and uniform dispersoids as well as high hardness.

From the hardness behavior observed in the Vickers hardness value (HV0,2) versus annealing temperature graph as in Figure 4, it is clear that both ODS ferritic steel samples in this present study approaches the thermal stability up to annealing temperature of 600°C and high hardness value up to annealing temperature of 800°C. With the uniform and ultra-fine incorporation of dispersoids within this material matrix, the thermal stability of this material could be enhanced up to 700°C and the hardness at various elevated temperature could be increased. This is because the performance of ODS ferritic steel at high temperature is recognized to depend on the dispersion state of oxides and its size as well.

#### CONCLUSION

In this present study, the effect of annealing to the hardness of high Y<sub>2</sub>O<sub>3</sub>-ODS ferritic steels has been investigated. XRD analysis showed the crystal structure of the samples which confirms the complete solution of Cr into Fe lattice and also the dispersion of Y<sub>2</sub>O<sub>3</sub> nanoparticles. FESEM characterization demonstrated the morphology of the samples which indicates the dispersion and incorporation state of dispersoids within the samples matrix. Vickers hardness test with a load of 200 gf has identified the hardness value of both samples as a function of annealing temperature. Vickers hardness value (HV0,2) versus annealing temperature graph showed the hardness behavior of the samples at various high temperature which is started to decrease at temperature of 600°C due to grain growth. The hardness value of both samples (1Y and 5Y) identified at this annealing temperature (600°C) is 855 HV0,2 and 808 HV0,2, respectively.



## ACKNOWLEDGEMENTS

The authors would like to acknowledge the Nuclear Science Programme, Universiti Kebangsaan Malaysia through Grant DIP-2014-022 and AP-2015-006 for the financial support given. The authors also acknowledge the Center for Research and Instrumentation Management (CRIM) at the Universiti Kebangsaan Malaysia for the facility support given.

## REFERENCES

- Alinger, M.J., Odette, G.R. & Lucas, G.E. 2002. Tensile and fracture toughness properties of MA957: Implications to the development of nanocomposited ferritic alloys. *Journal of Nuclear Materials* 307-311(Part 1): 484-489.
- Boulnat, X., Fabregue, D., Perez, M., Mathon, M.H. & de Carlan, Y. 2013. High temperature tensile properties of nano-oxide dispersion strengthened ferritic steels produced by mechanical alloying and spark plasma sintering. *Metallurgical and Materials Transactions A* 44: 2461-2465.
- Fischer, J.J. 1978. *Dispersion Strengthened Ferritic Alloy for Use in Liquid-Metal Fast Breeder Reactors (LMFBRs)*. US4075010A.
- Gelles, D.S. 1996. Microstructural examination of commercial ferritic alloys at 200 dpa. *Journal of Nuclear Materials* 233-237: 293-298.
- Hayashi, T., Sarosi, P.M., Schneibel, J.H. & Mills, M.J. 2008. Creep response and deformation processes in nanocluster-strengthened ferritic steels. *Acta Materialia* 56: 1407-1416.
- Hoeltzer, D.T., Bentley, J., Sokolov, M.A., Miller, M.K., Odette, G.R. & Alinger, M.J. 2007. Influence of particle dispersions on the high-temperature strength of ferritic alloys. *Journal of Nuclear Materials* 367-370(Part A): 166-172.
- Kim, T.K., Noh, S., Kang, S.H., Park, J.J., Jin, H.J., Lee, M.K., Jang, J. & Rhee, C.K. 2016. Current status and future perspective of advanced radiation resistant oxide dispersion strengthened steel (ARROS) development for nuclear reactor system applications. *Journal of Nuclear Engineering and Technology* 48: 572-594.
- Klueh, R.L., Maziasz, P.J., Kim, I.S., Heatherly, L., Hoelzer, D.T., Hashimoto, N., Kenik, E.A. & Miyahara, K. 2002. Tensile and creep properties of an oxide dispersion-strengthened ferritic steel. *Journal of Nuclear Materials* 307-311: 773-777.
- Li, Q., Parish, C.M., Powers, K.A. & Miller, M.K. 2014. Helium solubility and bubble formation in a nanostructured ferritic alloy. *Journal of Nuclear Materials* 445: 165-174.
- McClintock, D.A., Sokolov, M.A., Hoelzer, D.T. & Nanstad, R.K. 2009. Mechanical properties of irradiated ODS-EUROFER and nanocluster strengthened 14YWT. *Journal of Nuclear Materials* 392: 353-359.
- Miao, P., Odette, G.R., Yamamoto, T., Alinger, M. & Klingensmith, D. 2008. Thermal stability of nano-structured ferritic alloy. *Journal of Nuclear Materials* 377: 59-64.
- Miller, M.K. & Zhang, Y. 2011. Fabrication and characterization of APT specimens from high dose heavy ion irradiated materials. *Ultramicroscopy* 111: 672-675.
- Nuclear Energy Agency (NEA). 2014. *Technology Roadmap Update for Generation IV Nuclear Energy Systems*. Generation IV International Forum (GIF).
- Pei, H. 2013. On the structure-property correlation and the evolution of nano-features in 12-13.5% Cr oxide dispersion strengthened ferritic steels. PhD Thesis. Karlsruhe Institute for Technologies (Unpublished).
- Saber, M., Xu, W., Li, L., Zhu, Y., Koch, C.C. & Scattergood, R.O. 2014. Size effect of primary  $Y_2O_3$  additions on the characteristics of the nanostructured ferritic ODS alloys: Comparing as-milled and as-milled/annealed alloys using S/TEM. *Journal of Nuclear Materials* 452: 223-229.
- Susila, P., Sturm, D., Heilmaier, M., Murty, B.S. & Sarma, V.S. 2011. Effect of yttria particle size on the microstructure and compression creep properties of nanostructured oxide dispersion strengthened ferritic (Fe-12Cr-2W-0.5Y<sub>2</sub>O<sub>3</sub>) alloy. *Journal of Materials Science and Engineering A* 528: 4579-4584.
- Ukai, S., Harada, M., Okada, H., Inoue, M., Nomura, S., Shikakura, S., Asabe, K., Nishida, T. & Fujiwara, M. 1993. Alloying design of oxide dispersion strengthened ferritic steel for long life FBRs core materials. *Journal of Nuclear Materials* 204: 65-73.
- Ukai, S., Okuda, T., Fujiwara, M., Kobayashi, T., Mizuta, S. & Nakashima, H. 2002. Characterization of high temperature creep properties in recrystallized 12Cr-ODS ferritic steel claddings. *Journal of Nuclear Engineering and Technology* 39: 872-879.
- Williams, C.A., Unifantowicz, P., Baluc, N., Smith, G.D.W. & Marquis, E.A. 2013. The formation and evolution of oxide particles in oxide-dispersion-strengthened ferritic steels during processing. *Acta Materialia* 61: 2219-2235.
- Zakine, C., Prioul, C. & Francois, D. 1996. Creep behaviour of ODS steels. *Journal of Materials Science and Engineering A* 219(1-2): 102-108.

Farha Mizana Shamsudin\* & Shahidan Radiman  
Nuclear Science Programme, School of Applied Physics  
Faculty of Science and Technology  
Universiti Kebangsaan Malaysia  
43600 UKM Bangi, Selangor Darul Ehsan  
Malaysia

Yusof Abdullah  
Material Technology Group, Industrial Technology Division  
Malaysian Nuclear Agency, Bangi  
43000 Kajang, Selangor Darul Ehsan  
Malaysia

Nasri A. Hamid  
Center for Nuclear Energy, College of Engineering  
Universiti Tenaga Nasional  
Putrajaya Campus, Jalan Ikram UNITEN  
43000 Kajang, Selangor Darul Ehsan  
Malaysia

\*Corresponding author; email: farha90mizana@gmail.com

Received: 6 October 2016

Accepted: 13 June 2017